

Indian Institute of Technology Bombay

---

Department of Physics

## **A Simple Mechanistic Model of Sprout Spacing in Tumour-Associated Angiogenesis**

Project Report: Physics of Biological Systems (PH 549)

Presenter:

**Kanishk Modi**

Roll No: 22B1848

Guide:

**Prof.**

**Mithun Mitra**

**Reference:** B. Addison-Smith, D.L.S. McElwain and P.K. Maini. A simple mechanistic model of sprout spacing in tumour-associated angiogenesis. *Journal of Theoretical Biology* 250 (2008) 1–15.

---

# Contents

<b>1</b>	<b>Introduction</b>	<b>1</b>
<b>2</b>	<b>Development of Mathematical Model</b>	<b>2</b>
2.1	Model domain . . . . .	2
2.2	Assumptions for the model . . . . .	2
2.3	Governing Equations for $A$ and $I$ . . . . .	3
2.4	Non-dimensionalisation . . . . .	4
<b>3</b>	<b>Simulations</b>	<b>5</b>
3.1	Variation of $\beta$ . . . . .	5
3.2	Variation of Inhibitor Threshold . . . . .	6
3.3	Variation of Activator Decay rate . . . . .	6
3.4	Variation of Limbus length ( $1/2$ ) . . . . .	7
<b>A</b>	<b>Special Mathematical Functions</b>	<b>8</b>
A.1	Special integral function $E_n(x)$ . . . . .	8
A.2	Modified Bessel function of the second kind . . . . .	8

# Chapter 1

## Introduction

The paper being reviewed develops a simple mathematical model of sprout formation during the initiation of angiogenesis induced by tumours. **Angiogenesis** is the process of new blood vessel formation from existing blood vessels. The model is based on the idea that feedback regulation plays the dominant role to avoid unchecked sprouting at the initiation of angiogenesis. No chemical interaction between the proangiogenic and antiangiogenic factors is assumed.

It was observed that removal of a primary tumour often led to rapid growth of its previously dormant metastases. This started the search for endogenous antiangiogenic molecules. Even though these molecules are produced locally, they act at distant sites to prevent small masses of tumour from attaining vascularization. **Vascularization** is important for nutrients and oxygen supply to the cells which supports the unwanted growth of tumour cells.

Although proangiogenic factors are also produced by the primary tumour, it was suggested that the antiangiogenic molecules had a longer half-life in circulation, and so became the dominant effect at the site of distant metastases. The paper also discusses the specifics of the inhibitors (including names) which has been excluded from the report.

## Chapter 2

# Development of Mathematical Model

### 2.1 Model domain

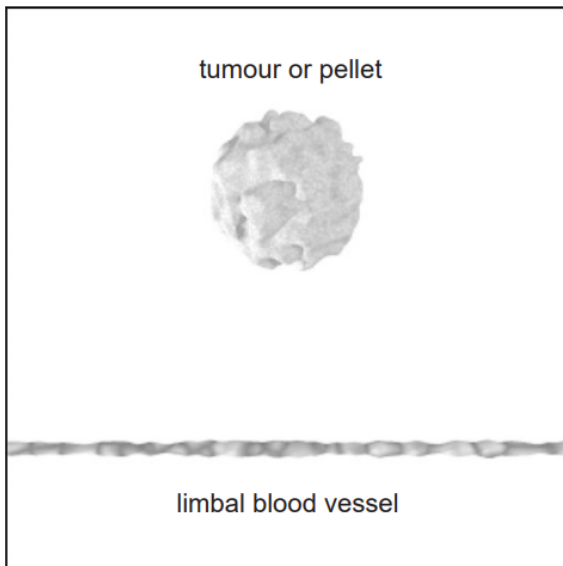


**Figure 2.1:** Schematic of the elements

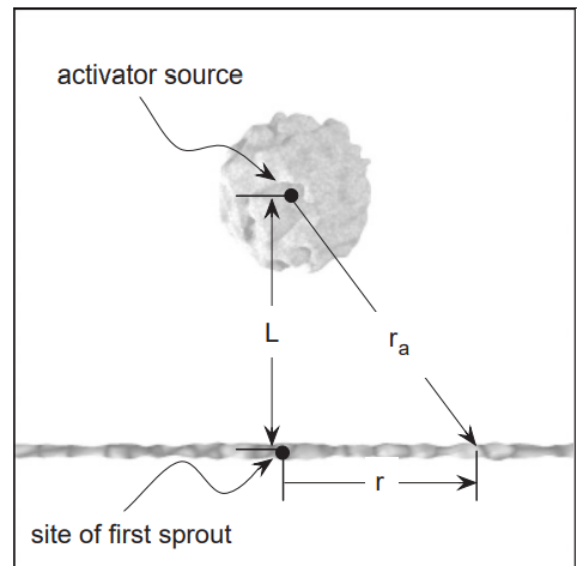


**Figure 2.2:** Measurement ref. system

The physical setup shown in Figure 1.1 and Figure 1.2 is based on an experimental angiogenesis model known as the **corneal pocket assay**. In this experiment, a pellet containing vascular endothelial growth factor (VEGF) is implanted into a pocket created in the avascular cornea of a mouse or a rabbit. This causes an angiogenic response in the periphery of the cornea nearest to the implantation.

Endothelial cells that line the blood vessels produce enzymes that degrade the membrane. Vessels nearby become hyperpermeable and plasma leaks out. Endothelial cell division is enhanced and cells migrate towards the source of angiogenic factor. Endothelial cells roll up and join together to form tubes. This process is called tubular morphogenesis. Further the tubes connect to form loops capable of circulating the blood.

### 2.2 Assumptions for the model

The pellet used for implantation in the corneal pocket assay is taken as a point source, located at a distance from the limbus (blood vessel) corresponding to the centre of the implant. The limbus is taken as a straight line at a perpendicular distance  $L$  from the point source. Figure

1.2 shows the polar coordinate system used. The axis is perpendicular to the plane containing the point source and limbus, and passes through the point source.

The model considers two species: an angiogenesis activator denoted by  $A$  (proangiogenic factor, e.g. VEGF) and an angiogenesis inhibitor denoted by  $I$  (antiangiogenic factor, e.g. endostatin, angiostatin). The activator is assumed to be produced continuously by the tumour and the inhibitor is assumed to be produced instantaneously at the initiation point of each new sprout. Let us remind that these two species do not interact in the discussed model.

Sprouts may form at any point on the existing limbal blood vessel subject to the following criteria:

- the activator concentration at that point must be greater than or equal to a chosen trigger value, i.e.  $A \geq A_{trig}$ .
- the inhibitor concentration at that point must be less than or equal to a chosen inhibitor threshold, i.e.  $I \leq I_{thresh}$ .

## 2.3 Governing Equations for $A$ and $I$

The pellet initializes the dynamics by releasing the activator in an empty domain. The first sprouting is at the closest point on the blood vessel, henceforth called the midpoint. Subsequently a 'puff' (instantaneous point source) of inhibitor is released. Sprouts further occur symmetrically about the line connecting the pellet and the blood vessel. Each new sprout releases a puff of inhibitor.

We account for the first order removal of the activator representing either a natural decay process or some other unknown kind of removal. For the angiogenic factor  $A$ , the governing equation thus becomes:

$$\frac{\partial A}{\partial t} = D_a \nabla^2 A - \lambda_a A \quad (2.1)$$

where  $D_a$  and  $\lambda_a$  are constants representing the diffusion and decay coefficients respectively. We attempt to solve the partial differential equation (PDE) for  $A(r_a, t)$  in an infinite 2D domain with radial symmetry, where  $r_a$  is the distance from the point source of strength  $q$ . Here, we have a continuous point source which we try to solve as an instantaneous point source integrated over time  $t$ . Integrating a constant continuous point source solution with respect to time gives:

$$A(r_a, t) = \frac{q}{4\pi D_a} \int_0^t \frac{1}{u} \exp\left(\frac{-r_a^2}{4D_a u} - \lambda_a u\right) du \quad (2.2)$$

We need to use numerical integration to solve for  $\lambda_a \neq 0$ . For  $\lambda_a = 0$ , i.e. when the decay is negligible, we have:

$$A(r_a, t) = \frac{q}{4\pi D_a} E_1\left(\frac{r_a^2}{4D_a t}\right) \quad (2.3)$$

where  $E_1(x)$  is the special integral function (Appendix A.1). There is no steady state of the activator for this case. For significant decay, we can have a steady state solution given as a modified bessel function of the second kind:

$$A(r_a) = \frac{q}{2\pi D_a} K_0\left(r_a \sqrt{\frac{\lambda_a}{D_a}}\right) \quad (2.4)$$

The governing equation for inhibitor can be written as a simple diffusion equation with a constant parameter  $D_i$  as the diffusion coefficient.

$$\frac{\partial I}{\partial t} = D_i \nabla^2 I \quad (2.5)$$

Now, for a single instantaneous point source, the boundary condition is given by a dirac delta function with a peak at  $r = 0$  and  $t = 0$ . For a single point source of strength  $p$ , the solution can be written as

$$I(r, t) = \frac{p}{4\pi D_i t} \exp\left(\frac{-r^2}{4D_i t}\right) \quad (2.6)$$

Each sprout will produce a new instantaneous point source of inhibitor. Let total number of sprouts be  $N_s$  with sprout  $n$  initiating at time  $t_n$ , at position  $r_n$ . The complete governing equation is now given as:

$$I(r, t) = \sum_{n=1}^{N_s} \frac{p}{4\pi D_i (t - t_n)} \exp\left(-\frac{(r - r_n)^2}{4D_i (t - t_n)}\right) H(t - t_n) \quad (2.7)$$

where  $H$  is the Heaviside function. Since there is no decay term, there is no steady state solution in infinite domain conditions.

## 2.4 Non-dimensionalisation

We rescale various quantities as follows to simplify our understanding of the model and simulate the sprouting along the limbus efficiently.

$$\begin{aligned} r^* &= \frac{r}{L}, & t^* &= \frac{t}{\tau}, & \tau &= \frac{L^2}{4D_a}, \\ A^* &= \frac{A}{\hat{A}}, & \hat{A} &= \frac{q\tau}{\pi L^2}, & I^* &= \frac{I}{\hat{I}}, \\ \hat{I} &= \frac{p}{\pi L^2}, & \beta &= \frac{D_i}{D_a}, & \gamma &= \lambda\tau \end{aligned}$$

The adopted renormalization gives:

$$A^*(r^*, t^*) = \int_0^{t^*} \frac{1}{u} \exp\left(\frac{-r_a^{*2}}{u} - \gamma u\right) du \quad (2.8)$$

$$I^*(r^*, t^*) = \sum_{n=1}^{N_s} \frac{1}{(t^* - t_n^*)} \beta \exp\left(-\frac{(r^* - r_n^*)^2}{t^* - t_n^*} \beta\right) H(t^* - t_n^*) \quad (2.9)$$

We proceed to simulating the positions of sprouts from the nearest point on the limbus by varying different parameters. At this point, it is important to remember that the sprouting is symmetrical in our model with respect to the nearest point.

## Chapter 3

# Simulations

[Github Repository](#) containing the code written is linked here.

The paper presents various different simulations. We focus on the sprout spacing with variation in parameters. For this, we use the non-dimensionalized equations of activator and inhibitor dynamics and simulate considering activator decay to be present. All assumed constant parameters have not been mentioned in the paper for each graph for which I have taken reasonable values giving mostly similar results. Further, I report the parameter being varied, assumed constants for the same in my simulations and compare with the graphs given in the paper. Unless the parameters are being varied, the following values have been taken for simulations:

$$\begin{aligned}\gamma &= 10 \\ \beta &= 1 \\ I_{th} &= 20 \\ r_{lim} &= 0.7 \\ t_1 &= 0.30306 \quad (\text{Time for the first sprout to appear}) \\ A_{th} &= 2 \times 10^{-5}\end{aligned}$$

### 3.1 Variation of $\beta$

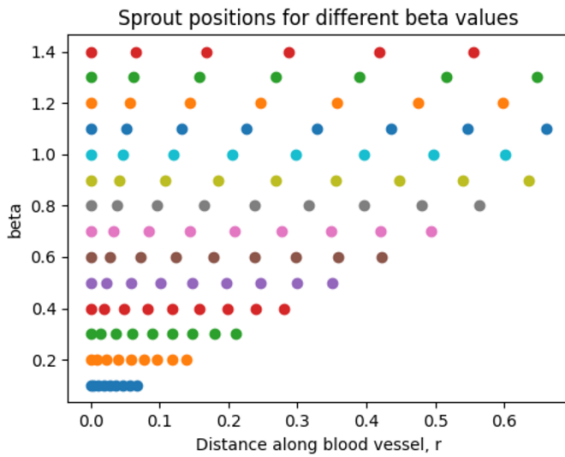


Figure 3.1: Simulated graph

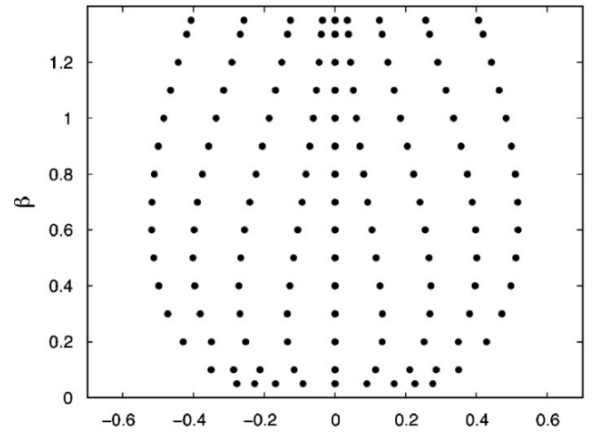


Figure 3.2: Paper presented graph

## 3.2 Variation of Inhibitor Threshold

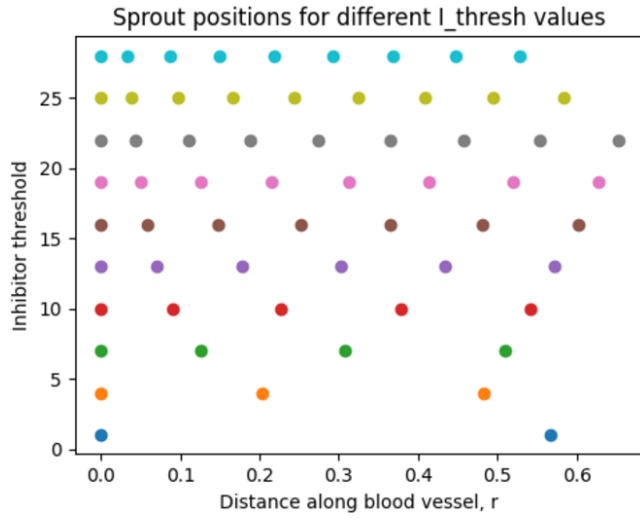


Figure 3.3: Simulated graph

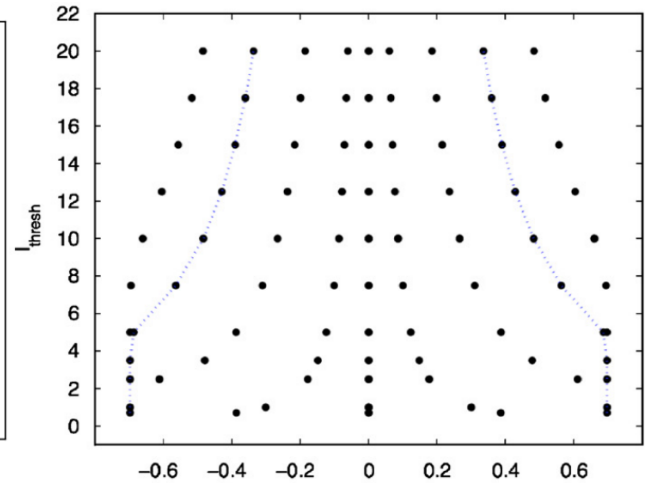


Figure 3.4: Paper presented graph

## 3.3 Variation of Activator Decay rate

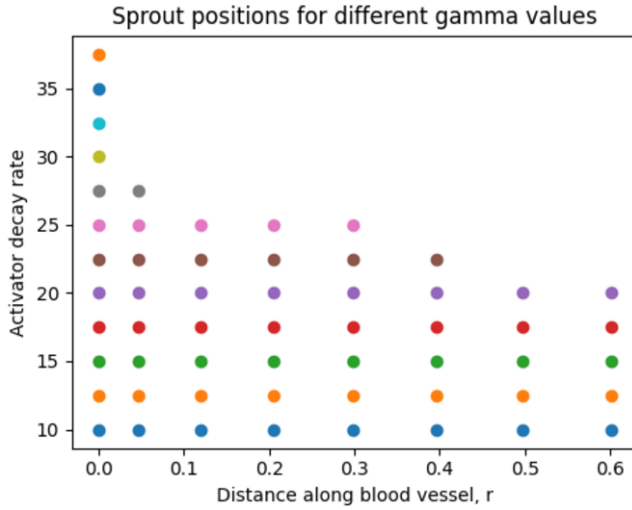


Figure 3.5: Simulated graph

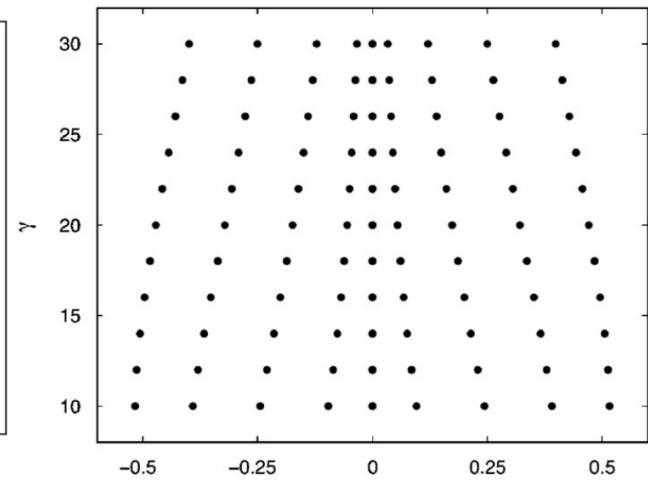


Figure 3.6: Paper presented graph

Last set is on next page.



### 3.4 Variation of Limbus length (1/2)

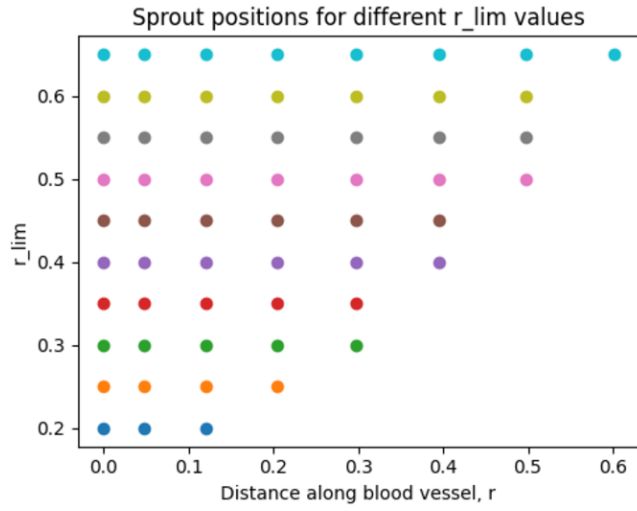


Figure 3.7: Simulated graph

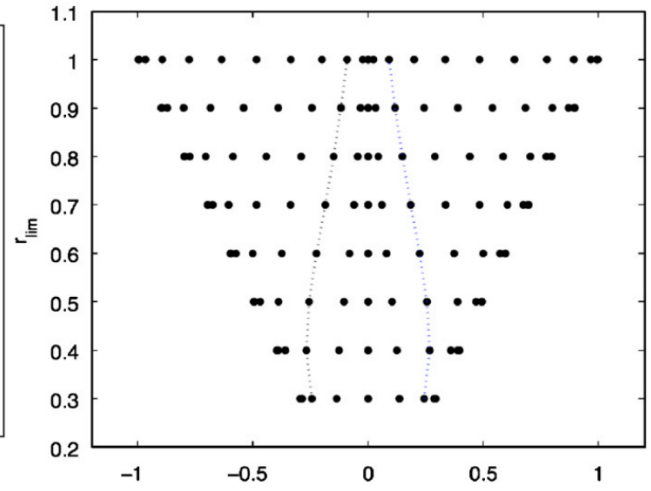


Figure 3.8: Paper presented graph

I presume that the major cause of differences is that I have assumed a particular activator trigger level which is not the case in the paper's final results. Since I have not covered the part where they stipulate the activator dependency on system parameters, I have not simulated taking the same into account.

## Appendix A

# Special Mathematical Functions

### A.1 Special integral function $E_n(x)$

The  $E_n(x)$  function is defined by the integral

$$E_n(x) \equiv \int_1^\infty \frac{e^{-xt} dt}{t^n} \quad (\text{A.1})$$

The special case  $n = 1$  gives

$$E_1(x) = \Gamma(0, x) \quad (\text{A.2})$$

where  $\Gamma(a, x)$  is the incomplete gamma function given by

$$\Gamma(a, x) = \int_x^\infty t^{a-1} e^{-t} dt \quad (\text{A.3})$$

$$\implies E_1(x) = \int_x^\infty \frac{e^{-u}}{u} du \quad (\text{A.4})$$

### A.2 Modified Bessel function of the second kind

The modified bessel functions of first ( $I_n(x)$ ) and second kind ( $K_n(x)$ ) are solutions of the modified bessel differential equation:

$$x^2 \frac{d^2 y}{dx^2} + x \frac{dy}{dx} - (x^2 + n^2)y = 0 \quad (\text{A.5})$$

An integral formula for  $K_n(x)$  is

$$K_n(x) = \frac{\Gamma\left(n + \frac{1}{2}\right) (2x)^n}{\sqrt{\pi}} \int_0^\infty \frac{\cos t dt}{(t^2 + x^2)^{n+\frac{1}{2}}} \quad (\text{A.6})$$

where  $\Gamma(z)$  is the gamma function given by

$$\Gamma(z) = \int_0^\infty t^{z-1} e^{-t} dt \quad (\text{A.7})$$

For  $n = 0$ , this integral formula simplifies to

$$K_0(x) = \int_0^\infty \frac{\cos(xt) dt}{\sqrt{t^2 + 1}} \quad (\text{A.8})$$

We proceed and focus on the case with activator decay. Since the solutions are not analytical, we simulate a part of the results given in the referenced paper.